Resonances in the Despin Dynamics of Dual-Spin Spacecraft

A. C. Or*
Hughes Aircraft Company, Los Angeles, California 90009

A unifying treatment of the nutation resonances encountered during the despin of platform of a dual-spin spacecraft with transverse inertia asymmetry and either platform or rotor imbalance is developed. The linear model equations governing the resonance dynamics depend on three nondimensional parameters that measure the degree of dynamic imbalance, asymmetry, and the time duration available for resonance growth. The solution dependence on all of these parameters is studied, and the basic physics of the phenomena is emphasized. The linear theory is supplemented by a simple variational analysis that provides a phase plane geometric interpretation of a rather interesting saddle-type transition, which has been observed in fully nonlinear simulations. The transition leads to an abrupt change in the spin orientation commonly known as the "stall" in spacecraft despin maneuvers.

Nomenclature

$\boldsymbol{H}$ = angular momentum vector of the system
H = magnitude of $\boldsymbol{H}$
H_3 = spin component of $\boldsymbol{H}$
$H_i^{(x)}$ = angular momentum component, $x = n$: nonresonant body; $x = r$: resonant body; $i = 1,2,3$
I_i = ith component total transverse moment of inertia, $i = 1,2$
I_3 = rotor moment of inertia, spin component
I_3^p = platform moment of inertia, spin component
I_{13} = rotor product of inertia
I_{13}^p = platform product of inertia
$I_i^{(x)}$ = moment of inertia referring to system reference frame, $x = n$: nonresonant body; $x = r$: resonant body; $i = 1,2,3$
$I_{ij}^{(x)}$ = product of inertia, $x = n$: nonresonant body; $x = r$: resonant body; $i = 1,2,3$
I_t = averaged total transverse moment of inertia
K = effective dynamic imbalance, nondimensional
L = Lagrange function
n_s = inertial nutation frequency
p,q,r,s = dimensionless parameters
T = external torque applied to the system
T_J = jet torque
T_M = internal motor torque
t = time, nondimensional time
α,β = dimensionless parameters defined in Eq. (9)
θ = cone angle, angle between axis 3 and $\boldsymbol{H}$
λ = Lagrange multiplier
μ = nondimensional dynamic asymmetry
σ_i = I_i/I_t, $i = 1,3$
σ_3^p = I_3^p/I_t
σ_{13} = I_{13}/I_t
τ = normalized time
τ_1 = normalized time at $t = 0$
ϕ = phase angle between axes 1 of the system frame and the nonresonant body
ω = transverse angular velocity vector
ω_0 = initial spin angular velocity of rotor and platform
ω_i = transverse angular velocity, component i, $i = 1,2$
ω_3 = rotor transverse angular velocity, spin component
ω_3^p = platform transverse angular velocity, spin component

Received May 15, 1989; revision received Jan. 12, 1990.

*Staff Engineer, Dynamics and Control Department. Member AIAA.

I. Introduction

GYROSCOPIC stiffness has often been used for stabilizing the attitude of a free-flying object against external overturning disturbances. For a single spinning body, this stiffness depends crucially on a certain asymmetry property expressed by the difference between the spin principal moment of inertia and the transverse principal inertia of the body. The stiffness vanishes as the difference tends to zero. As the stiffness vanishes, the spinning body reacts to disturbance overturning moments as if no spin stabilizing effect were present. Thus, in the design of spin-stabilized flying objects, this singularity condition is often avoided as far as possible. Unfortunately, for a dual-spin spacecraft (sometimes referred to as a Hughes hybrid gyrostat) undergoing a despin maneuver, this undesirable condition often occurs in the process. The condition can best be expressed as the resonance conditions, at which the inertial nutation frequency of the dual-spinner n_s coalesces with one of the spin speeds, either ω_3 or ω_3^p. When the difference in the principal transverse moments of inertia is small compared with the inertia values themselves, n_s is approximately a ratio of the total spin angular momentum magnitude to the total averaged transverse moment of inertia, measured about the overall center of mass. For a general reference on the attitude dynamics of dual-spin satellites, see Ref. 1. The resonance conditions can thus be expressed by the following simple form:

$$n_s \approx \frac{H_3}{I_t} = \sigma_3\omega_3 + \sigma_3^p\omega_3^p = \begin{cases} \omega_3^p & \text{when } \sigma_3 + \sigma_3^p < 1 \\ \omega_3 & \text{when } \sigma_3 + \sigma_3^p > 1 \end{cases} \tag{1}$$

where $H_3 = I_3\omega_3 + \omega_3^p$ is the spin angular momentum of the system. Since initially $\omega_3 = \omega_3^p = \omega_0$, during the despin, either one of the two resonance conditions expressed in Eq. (1) will occur, but not both. In other words, depending on whether the initial system spin moment of inertia is smaller or larger than the averaged system transverse inertia, the platform spin speed or the rotor spin speed will become equal to the inertial nutation frequency of the system at some instant during the despin.

The despin resonance dynamics of a dual-spin spacecraft has been studied in a number of papers.[2-6] Earlier work on the dual-spin spacecraft emphasized energy dissipation controls and nutation damper designs. The despin dynamics in the earlier work are also more focused on the particular spacecraft designs and configurations because the primary objectives for the studies were aimed at the success of the missions. Resonance due to the despin of an unbalanced platform for a dual-spin spacecraft with an asymmetric rotor was first reported in Scher and Farrenkopf's[2] simulation results. The phenomenon was then termed the resonance trap. Their study was followed by Cochran,[3] who provided a vigorous analysis

and a phase plane interpretation for the nonlinear motions by using the method of averaging. Similar problems in dual-spin spacecraft having more general mass properties and involving the spun up of an unbalanced platform were studied by Adams.[4] In addition to the resonance trap, Scher and Farrenkopf[2] also identified a minimum energy trap. The latter state is caused by the failure of the motor during the despin such that the bearing friction tends to settle the spacecraft at the all-spun state. This kind of minimum energy trap state was further studied by Hollars.[5] In a dual spinner, the platform is not distinguished from the rotor, except for the direction of spin angular momentum flux; it is conjectured that an unbalanced rotor might also cause the resonance. Lebsock et al.[6] studied the latter possibility and found yet another type of resonance, which they called the unitary inertia ratio resonance. A close examination of the results of the two types of resonances, however, shows very similar characteristics. Other than the resonance problems that typically involve the dynamic imbalances, considerable interest has also been devoted to stability analyses of despun dual-spin spacecraft. As examples, Tsuchiya and Saito[7] and Lukich and Mingori,[8] both treated the linear stability problem of a dual-spin spacecraft's on-axis equilibrium state (no nutation) by using the Floquet type methods. The spacecraft they studied possess asymmetry and static imbalance in both platform and rotor, but have no dynamic imbalance. Of particular interest are the stability diagrams they developed, which show the various stable and unstable parameter regimes.

The major purpose of this paper is to explore the physical foundations of the resonance phenomena. Thus, the emphasis is on the general behavior rather than on a particular spacecraft design or simulation. Furthermore, the full initial-value problem, rather than the linear stability problem about a certain equilibrium state, is solved. A simple spacecraft model is treated such that it allows for more simplified mathematics. A unifying treatment is provided for both the resonance trap due to platform imbalance and the unitary inertia ratio resonance due to the rotor imbalance. In the light of Eq. (1), however, the resonance trap and the unitary inertia ratio trap are more conveniently referred to as the platform and the rotor resonance [see, respectively, the upper and lower condition of Eq. (1)]. In Sec. II, the nondimensional model equations for both the rotor and platform resonances are derived. In Sec. III, solutions of the linearized model are sought, and their dependence on the parameters is studied. In Sec. IV, a phase plane interpretation of the resonance is briefly discussed by using a simple variational method. The stationary points on the analogy of the case of a single spinner are located and their stability characteristics are examined. For a reference on how the energy method can be applied to the spin-stabilized spacecraft dynamics, we refer readers to a paper by Likins.[9] In this paper, it is shown, unlike the case of a single spinner, that the energy added to and transferred between the spinning bodies allows the phase ellipsoids freedom to deform such that a transition across the separatrix of the saddle can occur and gives rise to a flat-spin nutation during despin. Finally, in Sec. V, a brief conclusion is given.

II. Mathematical Formulation

Figure 1 shows the geometric configuration of a dual-spin spacecraft, which consists of an asymmetric, statically balanced but dynamically unbalanced resonant body, and a symmetric, statically and dynamically balanced nonresonant body. The two bodies are connected by a single degree-of-freedom frictionless bearing and power transmission assembly (BAPTA). The resonant body can either be the rotor or the platform, depending on whether $\sigma_3 + \sigma_3^p$ is greater than or less than unity. During despin, the rotor and the platform are distinguished only by the direction of the spin angular momentum flux, which, in our terminology, is assumed only to flow from the platform to the rotor. The rotor is subject to a spin-up torque of $T_J + T_M$, whereas the platform is subject to a spin-down torque of $-T_M$. No delay in the turning on of T_J and T_M is assumed.

It is assumed that the system reference frame is rigidly attached to the resonant body, such that its origin is located at the system center of mass. Referring to the chosen frame, the angular momentum vector of the resonant body $\boldsymbol{H}^{(r)}$ and that of the nonresonant body $\boldsymbol{H}^{(n)}$ are expressed by

$$\boldsymbol{H}^{(r)} = \begin{bmatrix} I_1^{(r)} & I_{12}^{(r)} & I_{13}^{(r)} \\ I_{12}^{(r)} & I_2^{(r)} & I_{23}^{(r)} \\ I_{13}^{(r)} & I_{23}^{(r)} & I_3^{(r)} \end{bmatrix} \begin{pmatrix} \omega_1 \\ \omega_2 \\ \omega_r \end{pmatrix}$$

$$\boldsymbol{H}^{(n)} = \begin{bmatrix} I_1^{(n)}c^2 + I_{12}^{(n)}s^2 - 2I_{12}^{(n)}cs & (I_1^{(n)} - I_2^{(n)})cs + I_{12}^{(n)}(c^2 - s^2) & I_{13}^{(n)}c - I_{23}^{(n)}s \\ (I_1^{(n)} - I_2^{(n)})cs + I_{12}^{(n)}(c^2 - s^2) & I_2^{(n)}c^2 + I_1^{(n)}s^2 - 2I_{12}^{(n)}cs & I_{23}^{(n)}c + I_{13}^{(n)}s \\ I_{13}^{(n)}c - I_{23}^{(n)}s & I_{23}^{(n)}c + I_{13}^{(n)}s & I_3^{(n)} \end{bmatrix} \begin{pmatrix} \omega_1 \\ \omega_2 \\ \omega_n \end{pmatrix} \tag{2}$$

The moments of inertia of individual bodies are values referred to the system reference frame, rather than to the individual center of mass. Sub- and superscripts n and r denote the nonresonant and the resonant body, respectively. The short abbreviations c and s, respectively, denote $\cos\phi$ and $\sin\phi$, where ϕ is the angle between a transverse axis of an auxiliary reference frame that is also located at the system center of mass but is attached to the nonresonant body and the corresponding transverse axis of the system frame of reference. Thus, $\dot{\phi} = \omega_n - \omega_r$, and

$$(\omega_n, \omega_r) = \begin{cases} (\omega_3^p, \omega_3) & \text{for rotor resonance} \\ (\omega_3^p, \omega_3) & \text{for platform resonance} \end{cases} \tag{3}$$

We further assume

$$I_{12}^{(r)} = I_{12}^{(n)} = I_{23}^{(r)} = I_{23}^{(n)} = 0$$

The fully nonlinear numerical simulation results for the general despin problems do not indicate that any of the 12 products of inertia of individual bodies is important in the resonance; therefore, these can be safely dropped from the model. Furthermore, since the individual bodies are axisymmetric, by an appropriate choice of phases for the transverse axes of the system and auxiliary frames, both bodies' 23 components of product of inertia can be eliminated. For the subsequent simplifications of the model, it is assumed that both the dynamic imbalance and asymmetry of the individual body are small compared with the principal inertia values. Also, it is assumed that the nutation growth is small such that linearization is valid.

After substituting Eq. (2) into the equation of motion,

$$\dot{\boldsymbol{H}} + \boldsymbol{\omega} \times \boldsymbol{H} = \boldsymbol{T}$$

we obtain the following component equations,

$$(I_1^{(r)} + I_1^{(n)}c^2 + I_2^{(n)}s^2)\dot{\omega}_1 + (I_1^{(n)} - I_2^{(n)})cs\dot{\omega}_2 + I_{13}^{(n)}c\dot{\omega}_n + I_{13}^{(r)}\dot{\omega}_r + (\omega_2 H_3 - \omega_r H_2) + [2(I_2^{(n)} - I_1^{(n)})cs\omega_1 + (I_1^{(n)} - I_2^{(n)})(c^2 - s^2)\omega_2 - I_{13}^{(n)}s\omega_n](\omega_n - \omega_r) = 0 \tag{4a}$$

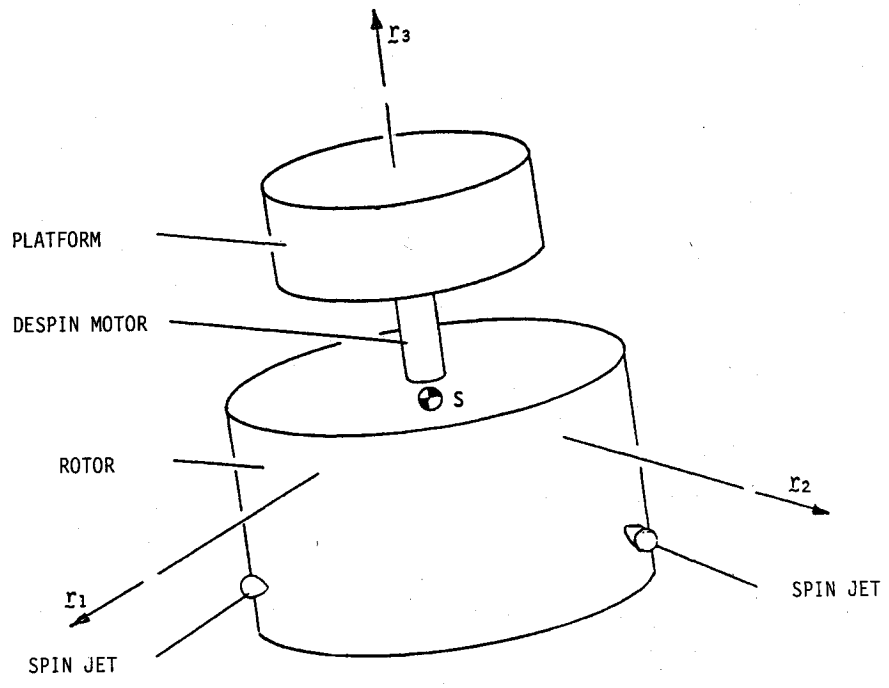

Fig. 1 The geometry of a dual-spin spacecraft.

$$(I_2^{(r)} + I_2^{(n)}c^2 + I_1^{(n)}s^2)\dot{\omega}_2 + (I_1^{(n)} - I_2^{(n)})cs\dot{\omega}_1 + I_{13}^{(n)}s\dot{\omega}_n + (\omega_r H_1 - \omega_1 H_3) + [2(I_1^{(n)} - I_2^{(n)})cs\omega_2 + (I_1^{(n)} - I_2^{(n)})(c^2 - s^2)\omega_1 + I_{13}^{(n)}c\omega_n](\omega_n - \omega_r) = 0 \quad (4b)$$

$$I_{13}^{(n)}c\dot{\omega}_1 + I_{13}^{(n)}s\dot{\omega}_2 + I_3^{(n)}\dot{\omega}_n + I_{13}^{(r)}\dot{\omega}_1 + I_3^{(r)}\dot{\omega}_r + (\omega_1 H_2 - \omega_2 H_1) + [-I_{13}^{(n)}s\omega_1 + I_{13}^{(n)}c\omega_2](\omega_n - \omega_r) = T_J \quad (4c)$$

On account of an additional degree of freedom between the bodies, Eq. (4c) can be split further into two component equations by considering the spin momentum balance of one of the two bodies. The two equations obtained are such that one holds for the resonant and the other for the nonresonant body,

$$I_{13}^{(r)}\dot{\omega}_1 + I_3^{(r)}\dot{\omega}_r + (\omega_1 H_2^{(r)} - \omega_2 H_1^{(r)}) = \begin{cases} T_J + T_M & \text{for rotor resonance} \\ -T_M & \text{for platform resonance} \end{cases} \quad (4d)$$

$$I_{13}^{(n)}(c\dot{\omega}_1 + s\dot{\omega}_2) + I_3^{(n)}\dot{\omega}_n + (\omega_1 H_2^{(n)} - \omega_2 H_1^{(n)}) [-I_{13}^{(n)}s\omega_1 + I_{13}^{(n)}c\omega_2](\omega_n - \omega_r) = \begin{cases} -T_M & \text{for rotor resonance} \\ T_J + T_M & \text{for platform resonance} \end{cases} \quad (4e)$$

Assuming a symmetric and balanced nonresonant body, we have

$$I_1^{(n)} = I_2^{(n)}, \qquad I_{13}^{(n)} = 0$$

which allows Eqs. (4a), (4b), (4d), and (4e) to be simplified to the following system that does not involve time-varying coefficients

$$I_1\dot{\omega}_1 + I_{13}^{(r)}\dot{\omega}_r + (H_3 - I_2\omega_r)\omega_2 = -I_{13}^{(r)}\omega_1\omega_2 \quad (5a)$$

$$I_2\dot{\omega}_2 - (H_3 - I_1\omega_r)\omega_1 = -I_{13}^{(r)}(\omega_r^2 - \omega_1^2) \quad (5b)$$

$$I_3^{(r)}\dot{\omega}_r + I_{13}^{(r)}\dot{\omega}_1 + (I_2 - I_1)\omega_1\omega_2 - I_{13}^{(r)}\omega_2\omega_r = \begin{cases} T_J + T_M & \text{for rotor resonance} \\ -T_M & \text{for platform resonance} \end{cases} \quad (5c)$$

$$I_3^{(n)}\dot{\omega}_n = \begin{cases} -T_M & \text{for rotor resonance} \\ T_J + T_M & \text{for platform resonance} \end{cases} \quad (5d)$$

In Eqs. (5), I_1 and I_2 denote the system transverse moment of inertia. From Eqs. (5), the model equations for the rotor resonance and the platform resonance are derived after nondimensionalization and linearization.

A. Rotor Resonance

Certain terms in Eqs. (5) can be neglected based on our model assumptions. In Eq. (5a), $I_{13}\dot{\omega}_3(I_{13}^{(r)} = I_{13})$ can be neglected since its ratio to the first term is bounded by $I_{13}(\sigma_3 + \sigma_3^p)/I_1$, which is a small quantity since $I_{13} \ll I_1$ and $\sigma_3 + \sigma_3^p$ is of order unity. The nonlinear term on the right side is quadratic in the transverse rate, which is small if the nutation angle is small, and therefore can be neglected. Likewise, the nonlinear term $I_{13}\omega_1^2$ in the Eq. (5b) can be neglected. The same arguments apply to terms $I_{13}\dot{\omega}_1$, $(I_2 - I_1)\omega_1\omega_2$, and $I_{13}\omega_2\omega_3$ so that they can also be neglected. We introduce the platform despun time $(I_3^p\omega_0)/T_M$, the initial angular rate ω_0, and the averaged transverse inertia $I_t = (I_1 + I_2)/2$ as the scales for time, angular velocity, and self-inertia values. For convenience, the notations on the dimensionless variables will be kept the same as those of the dimensional with no confusions. From Eqs. (3) and (5), we may write the nondimensional platform and rotor spin component equations, in terms of the scaled variables, as

$$\omega_3^p = 1 - t, \qquad \omega_3 = 1 + \beta t \quad (6)$$

where

$$\beta = (1 + T_J/T_M)(I_3^p/I_3) \quad (7)$$

By substituting Eqs. (6) into the transverse component equation of Eqs. (5), we obtain

$$\dot{\omega}_1 + \alpha(p - qt)\omega_2 + \Delta\alpha(r + st)\omega_2 = 0 \tag{8a}$$

$$\dot{\omega}_2 - \alpha(p - qt)\omega_1 + \Delta\alpha(r + st)\omega_1 = \hat{K}(t) \tag{8b}$$

The nondimensional parameters that appear in Eqs. (8) are defined as follows:

$$\alpha = (I_3\omega_0^2)/T_M, \qquad \Delta\sigma_1 - 1 = 1 - \sigma_2, \qquad p = (\sigma_3 + \sigma_3^p - 1)$$

$$q = (1 - \sigma_3)\beta + \sigma_3^p, \qquad r = 2 - (\sigma_3 + \sigma_3^p)$$

$$s = (2 - \sigma_3)\beta + \sigma_3^p, \qquad \hat{K}(t) = \sigma_{13}\alpha(1 + \beta t)^2 \tag{9}$$

where σ_i is the ith component of inertia ratio, i.e., the inertia scaled by I_t. The derivation of Eqs. (8) has also made use of the assumption that $\Delta \ll 1$. Note that the identities $p + r \equiv 1$ and $q + \beta \equiv s$ hold. The signs of the parameters are such that α is positive; Δ is positive by the definition that $I_1 > I_2$; p is positive because it is a necessary condition for the rotor resonance; r is non-negative from the definition of moment of inertia; q is negative only when $\sigma_3 > 1 + T_M/T_J$, which is unrealizable for realistic spacecraft mass properties where typically $\sigma_3 < 1$, thus, q is assumed positive; these identities show that s is positive if q is positive. Equations (8) can further be simplified by a shift in time. Define $\tau = (\alpha q)^{1/2}(t - t_c)$, where $t_c = p/q$. In terms of τ, the normalized equations then appear as

$$\frac{d}{d\tau}\omega_1 + (-\tau + \mu)\omega_2 = 0, \qquad \frac{d}{d\tau}\omega_2 + (\tau + \mu)\omega_1 = K \tag{10}$$

where τ varies from $\tau_1 = -(p/q)(\alpha q)^{1/2}$ to $\tau_2 = (1 - p/q)(\alpha q)^{1/2}$, and

$$\mu = \Delta(\alpha/q)^{1/2}[r + (sp)/q], \qquad K = -\sigma_{13}(\alpha/q)^{1/2}[1 + (\beta p)/q]^2 \tag{11}$$

In these equations, $\hat{K}(t)$ has been replaced by $\hat{K}(t_c)$ and is denoted by K. Such simplification is based on the fact that $\hat{K}(t)$ varies on a much slower time scale in the proximity of the resonance, as compared to the growth rate time scales of ω_1 or ω_2, thus, $\hat{K}$ can be effectively treated as constant. Model equations similar to Eqs. (10) were first derived in Ref. 3 by using a different scaling. The normalized form of Eqs. (10) has the advantage that it depends on minimal numbers of parameters, which makes a thorough parametric analysis possible. The solution dependence on the physical parameters of the spacecraft can easily be deduced by using the relationships of Eqs. (9).

B. Platform Resonance

The same scalings as in the rotor resonance are introduced. By the same arguments, the following terms are dropped from Eqs. (5): $I_{13}^p\dot{\omega}_3^p$, $-I_{13}^p\omega_1\omega_2$, $I_{13}^p\omega_1^2$, $I_{13}^p\dot{\omega}_1$, $(I_2 - I_1)\omega_1\omega_2$, and $I_{13}^p\omega_2\omega_3^p$. The nondimensional spin component equations are still given by Eqs. (6) and (7), and the transverse equations are still given by Eqs. (8). Certain quantities in Eqs. (9) are, however, to be redefined. Although the expressions for α, Δ, and r remain the same, the other quantities reappear as follows:

$$p = (\sigma_3 + \sigma_3^p - 1), \qquad q = (-1 - \sigma_3\beta) + \sigma_3^p$$

$$s = (-2 - \sigma_3\beta) + \sigma_3^p, \qquad \hat{K}(t) = -\sigma_{13}^p\alpha(1 - t)^2 \tag{12}$$

The following identities $p + r \equiv 1$, $q \equiv s + 1$ apply. With a parallel reasoning to that for the rotor resonance case, here p, q, and s assume negative values. The transverse equations are further simplified by a shift in time by redefining $\tau = (-\alpha q)^{1/2}(t - t_c)$, where $t_c = p/q$. In terms of τ, the normalized equations are

$$\frac{d}{d\tau}\omega_1 + (\tau + \mu)\omega_2 = 0, \qquad \frac{d}{d\tau}\omega_2 + (-\tau + \mu)\omega_1 = K \tag{13}$$

where τ varies from $\tau_1 = -(p/q)(-\alpha q)^{1/2}$ to $\tau_2 = (1 - p/q)(-\alpha q)^{1/2}$, and

$$\mu = \Delta(-\alpha/q)^{1/2}[r + (sp)/q], \quad K = -\sigma_{13}^p(-\alpha q)^{1/2}(1 - p/q)^2 \tag{14}$$

III. Linear Model Results

To specify a complete initial-value problem, we assume $\tau = \tau_1$, or $\tau = 0$, as the initial condition, where

$$\omega_2 = 0, \quad \omega_1 = \begin{cases} K/(\tau_1 + \mu) & \text{for rotor resonance} \\ K/(-\tau_1 + \mu) & \text{for platform resonance} \end{cases} \tag{15}$$

These initial conditions represent the wobble solutions at which both $\dot{\omega}_1$ and $\dot{\omega}_2$ vanish. The initial-value problem defined by Eqs. (10) and (15) and (13) and (15) pose two very similar three-parameter systems that can be treated as one generalized problem through a variable transformation. The three parameters of the system are 1) the initial time parameter τ_1, which measures the duration between the start of despin and the peak transverse rate growth; 2) the dynamic imbalance parameter K, which measures the unbalanced effects of mass properties on the resonance; and 3) the dynamic asymmetry parameter μ, which appears to amplify the resonance. For the linear problem, the parameter K can be eliminated by a rescaling of the dependent variables. Thus, a change of sign in K, or I_{13}, implies a change of sign in the transverse rates. The system does not admit a simple closed-form solution. In Ref. 6, the authors showed that closed-form solutions indeed exist and are obtainable through the method of factoring. Unfortunately, the form of the solutions is rather complicated. For our purpose, solutions are obtained through a standard initial-value solver called the advanced continuous simulation language (ACSL).[10]

As noted earlier, Eqs. (10) and (13) can be treated as identical in the light of the following transformation

$$\begin{pmatrix} \omega_1 \\ \omega_2 \end{pmatrix} \to \begin{pmatrix} -\omega_1 \\ \omega_2 \end{pmatrix}, \qquad \mu \to -\mu \tag{16}$$

The transformation reduces one system of equations to the other. This property is inherent in the symmetry properties of the physical configuration and suggests that only one of the two sets of equations has to be dealt with. Caution is advised, however, since appropriate definitions of the non-dimensional parameters and initial condition for the type of resonance must be used.

In Figs. 2–4, we present the simulation results. Figures 2 shows the nondimensional transverse rates vs time, in the case of rotor resonance, for $\tau_1 = -5.6$, and $K = 1$. Since K can be scaled into the rates, the curves actually show ω_1/K and ω_2/K. Figure 2a has $\mu = -1.0$ and Fig. 2b has $\mu = 1.0$. The amplitude, $|\omega| = (\omega_1^2 + \omega_2^2)^{1/2}$, typically grows from the value given by Eqs. (15) to a maximum value and then settles to a residual fluctuation with a mean value smaller than the peak value. The case where $\mu = 1$ has been compared with the result of Ref. 4 and the agreement is reasonably good. By means of the transformations of Eqs. (16), the transverse angular rates for the platform resonance can also be found from the curves. An interesting feature of the solutions is that the amplitude of the transverse rate is asymmetric with respect to the sign of μ. This property is illustrated in Fig. 3 for the case of rotor resonance, which shows the peak (upper curve) and the mean residual (lower curve) value of $|\omega/K|$ (or equivalently, of $|\omega|$ for $K = 1$) vs μ. The initial time parameter τ_1 is chosen equal to -5.1. For μ positive, there appears to be a dramatic divergence in both the peak and the mean residual amplitudes as μ

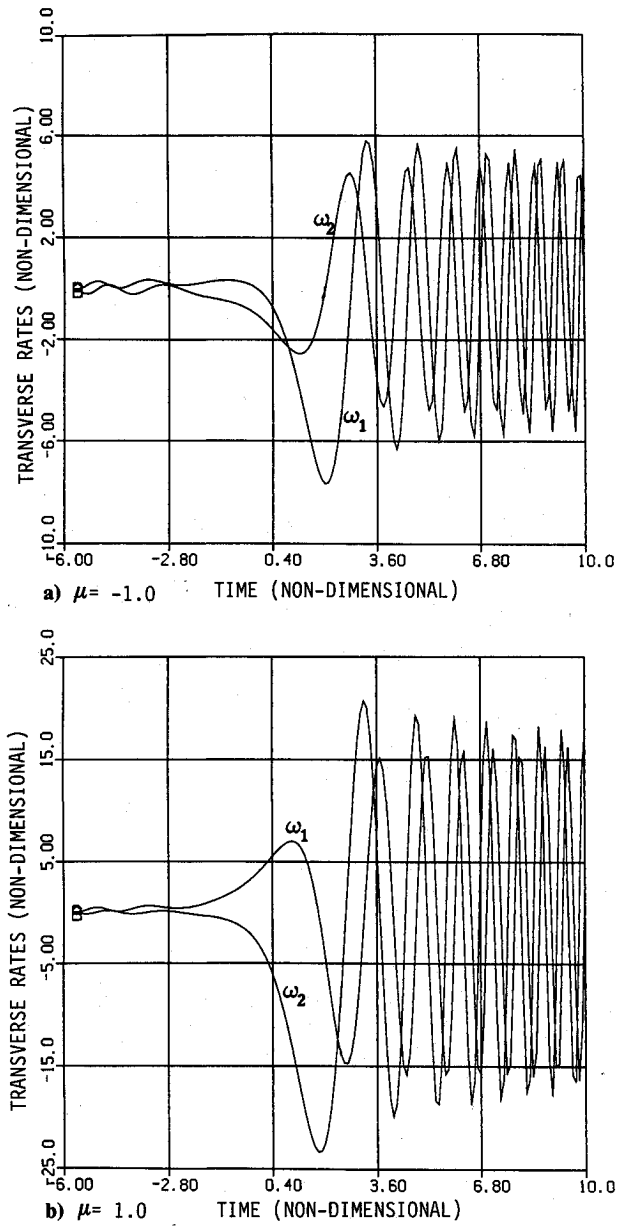

Fig. 2 The non-dimensional transverse angular rates vs time in the case of rotor resonance.

exceeds a value of about 0.75. This rapid variation with μ makes the analytical properties of Eqs. (13) particularly interesting, but also warrants that a regular perturbation expansion about $\mu = 0$ is in general invalid except for $\mu \ll 1$. Thus, the sign of μ affects the amplitude substantially. This result leads us to conclude that the larger maximal resonant growth occurs when the product of inertia lies in the plane containing the bearing axis and the axis corresponding to the larger of I_1 and I_2. For the platform resonance, on the other hand, Eqs. (16) suggest that the larger maximal growth occurs when the product of inertia lies instead in the plane containing the bearing axis and the smaller of the two transverse inertia. Figure 4 shows the dependence of the transverse rate amplitude $|\omega/K|$ on the initial time parameter τ_1 for the case of rotor resonance. The curves shown are such that the upper set corresponds to the case of $\mu = 1.0$ and the lower set corresponds to the case of $\mu = 0.57$. In each set, the upper and the lower curves again correspond, respectively, to the peak and mean residual values. Of interest is that the curves qualitatively appear like a reflection about the vertical axis of the curves showing the transverse rate amplitude vs time. The peak and residual values are well correlated. The maximum of all the local maxima is the closest peak to $\tau_1 = 0$. By utilizing the transformation of Eqs. (16), the corresponding results for the platform resonance can be obtained accordingly from Figs. 2–4.

IV. Simple Variational Method

A geometric view of the phase portrait of the resonance dynamics is desirable since it leads to a better physical understanding of the problem. However, since many solutions may be required for a complete description of the different behaviors in different parameter regimes, the full simulation approach can be very laborious. The variational approach, on the other hand, can provide a simple portrait, or in some cases, can even yield useful results, but the method is more restrictive as it is often found only applied to single spinning bodies (see Ref. 11, for example). For a dual spinner in which both energy and momentum are conserved, the energy and the angular momentum ellipsoids are described by a four-dimensional, rather than a three-dimensional, phase space. The rate state that constitutes the phase space consists of components ω_1, ω_2, ω_3, and ω_3^p. The ellipsoids slowly deform in the phase space as the motor torque and the jet torque simultaneously add kinetic energy and angular momentum to the system (loss due to mass ejection is negligible for our consideration). As Kane and Levinson[12] reported, however, care must be taken in applying the method to realistic systems since these systems are nonconservative. Here, we are only interested in the loca-

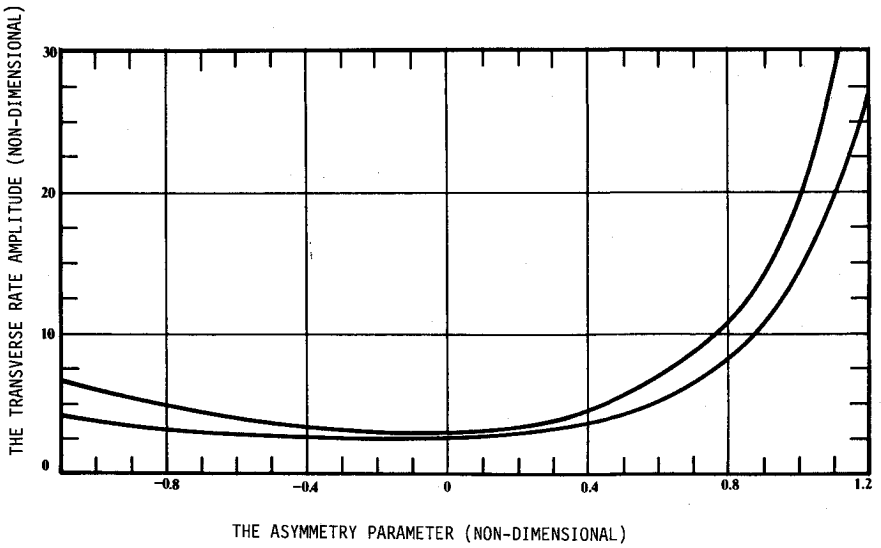

Fig. 3 The peak and mean residual transverse rate amplitudes vs the asymmetry parameter.

tions of stationary points in the space and their stability properties. Results will be compared with the simulation's to ensure validity. Of particular interest is the transition through a "saddle," triggered by large coning, that causes a sudden change of the spin orientation. In the spacecraft mission terminology, this transition is commonly referred to as the "stall."

The angular momentum magnitude squared and the kinetic energy for a dual spinner are

$$H^2 = I_1^2\omega_1^2 + I_2^2\omega_2^2 + (I_3\omega_3 + I_3^p\omega_3^p)^2 \tag{17a}$$

$$2T = I_1\omega_1^2 + I_2\omega_2^2 + I_3\omega_3^2 + I_3^p(\omega_3^p)^2 \tag{17b}$$

Assuming a stationary system, we can extremize the energy by constraining the angular momentum. To do this we define a Lagrange function L

$$L = (I_1\omega_1^2 + I_2^2\omega_2^2 + I_3\omega_3^2 + I_3^p\omega_3^{p2}) + \lambda[H^2 - I_1^2\omega_1^2 - I_2^2\omega_2^2 - (I_3\omega_3 + I_3^p\omega_3^p)^2] \tag{18}$$

where λ is the associated Lagrange multiplier. Note that it is also valid to extremize H by constraining T instead of redefining λ. The condition for the existence of an equilibrium and its stability are determined, respectively, by the vanishing of the first derivative and by inspecting the sign of the second derivative in the Taylor expansion of L. Thus, $\delta L = 0$ gives rise to four component equations. Each corresponds to the vanishing of a partial derivative,

$$I_1\omega_1(1 - \lambda I_1) = I_2\omega_2(1 - \lambda I_2) = 0 \tag{19a}$$

$$I_3\omega_3(1 - \lambda I_3) - \lambda I_3 I_3^p\omega_3^p = 0 \tag{19b}$$

$$I_3^p\omega_3^p(1 - \lambda I_3^p) - \lambda I_3 I_3^p\omega_3 = 0 \tag{19c}$$

Equations (18) and (19) determine the set of all possible stationary points. The stability of these equilibria can be examined from the signs of the term $\delta^2 L$,

$$\delta^2 L = \frac{1}{2}\sum_{i=1}^{3}\left[\frac{\partial^2 F}{\partial\omega_i^2}(\omega_i - \omega_i^{(s)})^2 + \frac{\partial^2 F}{\partial\omega_i^{p2}}(\omega_i - \omega_i^{p(s)})^2\right] \tag{20}$$

where superscript s refers to the stationary values. Equation (20) can be greatly simplified because all of the mixed derivatives vanish. From Eqs. (19), four stationary points can be immediately located. These are

$$\omega_2 = \omega_3 = \omega_3^p = 0, \quad H^2 = I_1^2\omega_1^2, \quad 2T = I_1\omega_1^2 \tag{21a}$$

$$\omega_1 = \omega_3 = \omega_3^p = 0, \quad H^2 = I_2^2\omega_2^2, \quad 2T = I_2\omega_2^2 \tag{21b}$$

$$\omega_1 = \omega_2 = \omega_3^p = 0, \quad H^2 = I_3^2\omega_3^2, \quad 2T = I_3\omega_3^2 \tag{21c}$$

$$\omega_1 = \omega_2 = \omega_3 = 0, \quad H^2 = (I_3^p)^2(\omega_3^p)^2, \quad 2T = I_3^p(\omega_3^p)^2 \tag{21d}$$

Analogous to the single-body case, the two stationary points that are associated with the largest and smallest moment of inertia are vortex points where $\delta^2 L = 0$. These equilibria are Lyapunov stable. The other two stationary points are associated with the intermediate moments of inertia and are saddles. These equilibria admit both positive and negative $\delta^2 L$, depending on the direction of the derivative taken, and therefore are unstable. Although the saddles might be of interest, a close examination of the trajectories of the phase state of despin suggests, however, that none of these equilibria actually come close to the despin state. Examining the phase state trajectories, we conclude that in fact the state space is effectively three dimensional for the following reason: various nonlinear simulation results have consistently shown that ω_n is approximately proportional to time even under the very large coning motion of the spinner. This property is apparent from Eq. (5d). Indeed, the nonlinear effects only appear to affect ω_r. Thus, ω_n can be treated effectively as a prescribed parameter of time. This allows us to drop from Eqs. (19) the equation that represents the vanishing of the partial derivative of ω_n. Now, the remaining three equations of Eqs. (19) can still be solved for the three remaining variables, after one of the four components has been prescribed. Solutions to the latter set of problems will be called quasistationary. In a strict sense, they are not true equilibria because now the system is time varying. Their importance lies in the possibility that these extrema may prompt the state trajectory to change characteristics when the latter comes close enough to their proximity.

To see how this can actually happen, first, let us consider the case of rotor resonance. Equation (19c) is dropped. From the linear results, Fig. 2 shows that for μ positive (negative), the maximum growth occurs with a negative ω_2 (ω_1) where ω_1 (ω_2) vanished. Since the full simulations show that a change of

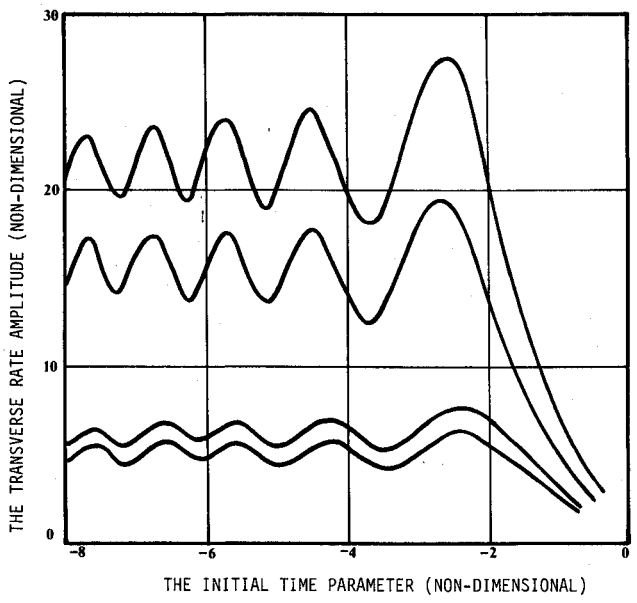

Fig. 4 The peak and mean residual transverse rate amplitudes vs the initial time parameter.

trajectory characteristics often occurs at the maximum of the transverse rate amplitude, the phase relationship will be used as a condition to be satisfied by Eqs. (19). Thus, for $I_1 > I_2$, or μ positive, Eqs. (19) are satisfied by

$$\omega_1 = 0, \qquad \omega_2 = \pm\left[\left(\frac{H}{I_2}\right)^2 - \left(\frac{I_3^p \omega_3^p}{I_2 - I_3}\right)^2\right]^{1/2}$$

$$\omega_3 = \left(\frac{I_3^p}{I_2 - I_3}\right)\omega_3^p, \qquad \omega_3^p = \omega_0 - \frac{T_M t}{I_3^p} \tag{22a}$$

where $\lambda = 1/I_2$. The last of the equations is just a slightly different form of Eqs. (6). For $I_1 < I_2$, or μ negative, we have instead

$$\omega_1 = \pm\left[\left(\frac{H}{I_1}\right)^2 - \left(\frac{I_3^p \omega_3^p}{I_1 - I_3}\right)^2\right]^{1/2}, \qquad \omega_2 = 0$$

$$\omega_3 = \left(\frac{I_3^p}{I_1 - I_3}\right)\omega_3^p, \qquad \omega_3^p = \omega_0 - \frac{T_M t}{I_3^p} \tag{22b}$$

where $\lambda = 1/I_1$. For the last pair of equations in Eqs. (22a) or (22b) to be consistent, we also require

$$\frac{I_3^p}{I_i - I_3} > 1 \qquad i = 1 \text{ for } I_1 < I_2, \quad i = 2 \text{ for } I_1 > I_2 \tag{22c}$$

Only when Eqs. (22a) and (22c) or (22b) and (22c) are satisfied can the quasistationary point exist. The position of the point in the phase space is completely determined by the spin rate of the nonresonant body since H can be specified as a known function of time. At first sight, the condition specified by the third equation of Eqs. (22a) or (22b) appears difficult to reach since in the despin ω_3 increases while ω_3^p decreases. The spin rate behavior is, however, altered by the pronounced nonlinearity. In fact, what the linear theory failed to predict is when the transverse rate amplitude becomes on the same order of magnitude as the spin rates. The nonlinear solutions actually show that ω_r not only ceases to grow, but actually decreases. Such an unusual saturation effect allows the possibility for the third equation to be satisfied simultaneously with the fourth equation near the instant of peak coning growth.

The stability equation is

$$\delta^2 L = \tfrac{1}{2}[I_1(1 - \lambda I_1)(\omega_1 - \omega_1^{(s)})^2 + I_2(1 - \lambda I_2)(\omega_2 - \omega_2^{(s)})^2 + I_3(1 - \lambda I_3)(\omega_3 - \omega_3^{(s)})^2] \tag{23}$$

with the appropriate λ value, depending on the sign of μ. By substituting Eqs. (22a) or (22b) into Eq. (23), it is found that the first two terms on the right of Eq. (23) are such that one vanishes and the other is negative. The third term is positive for $I_3 < \min[I_1, I_2]$. The latter inequality has to be satisfied in order that the rotor resonance occurs. Thus, we conclude that the quasistationary point is a saddle. Physically, the transition of the trajectory through a saddle corresponds to a switch over of the precession orientation: from precessing about the axial axis to precessing about the transverse axis of the larger moment of inertia. This transition can occur rapidly converting the dual-spin spacecraft into a stable flat spinner if given some energy dissipations. Fig. 5 provides an example of the fully nonlinear numerical simulation for the case of rotor resonance on how a switch over can actually occur by gradually increasing the asymmetry. The physical parameters used in the simulation are $T_M = 4$ ft-lbf, $T_J = 9.94$ ft-lbf; $I_3 = 4130$, $I_3^p = 1890$, $I_{13} = 4.0$, and all inertia in slug-ft^2. Running down from the top of the figure, I_1 and I_2 are, respectively, 5113.75 and 4872.25, 5113.775 and 4872.225, 5113.778 and 4872.222, 5113.800 and 4872.200, and, finally, 5114.500 and 4871.500. The averaged inertia I_t is fixed. This result indicates a very sensitive dependence on the asymmetry as the switch point is approached. The transition is observed to occur somewhere between the second and third rows of Fig. 5. In the figure, the left column shows the transverse rates ω_1 (solid) and ω_2 (dotted) in radians per second vs time in 10^3 s. The middle column

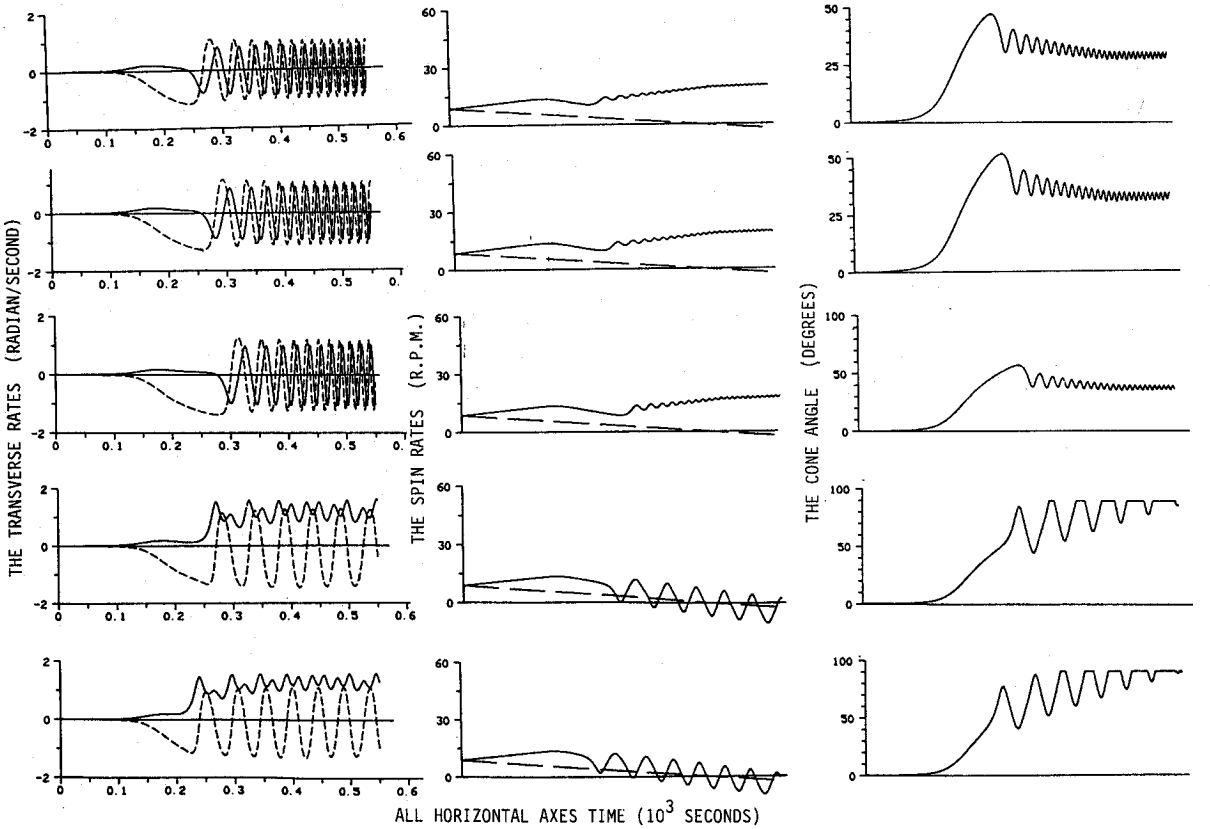

Fig. 5 A saddle-type transition in rotor resonance for a fixed imbalance and by a gradual increase of asymmetry.

Table 1 Comparison between the simulated and analytical values of the stall rate

I_1	I_2	I_3	I_3^p	I_{13}	t	ω_0	ω_1	ω_2	ω_3	ω_3^p	θ
5113.8	4872.0	4130.0	1890.0	4.0	255.0	0.916	0.0	−1.26	1.01	0.38	51.1
							0.0	−1.27	0.93	0.38	53.6
5047.2	4938.8	4130.0	1890.0	16.0	270.0	0.916	0.0	−1.34	0.87	0.34	57.5
							0.0	−1.35	0.81	0.34	59.1
5265.0	4720.9	4130.0	1890.0	4.0	195.0	0.524	0.0	−0.93	0.42	0.11	66.1
							0.0	−0.93	0.36	0.11	68.9

shows the spin rates ω_3 (solid) and ω_3^p (dotted) in revolutions per minute, vs time on the same scale. The right column shows the cone angle in degree vs time, also on the same scale. The cone angle is defined as the angle between the bearing axis and the system angular momentum vector. Running down from the top again, the maximal cone angle values in degrees are 47.1, 51.4, 56.9, 90.0, and 90.0. The figure shows that the nonlinear effects are so pronounced that actually ω_3 decreases, whereas ω_3^p, as suggested, is proportional to time. Without the nonlinear coupling, such a transition is unlikely to occur. Table I further shows a comparison of the simulation values at the switch over with the analytical values obtained from Eqs. (22a). Again the units are inertia in slug-ft^2, time in seconds, angular rates in radians per second, and cone angle in degrees. From the pairs of values that appear, the upper values correspond to that obtained from the full simulations and the lower values are calculated from the Eqs. (22a). The agreement appears reasonably good (within 8%).

Second, let us consider the platform resonance. Now, Eq. (19c) has to be dropped instead. For $I_1 > I_2$, or $\mu > 0$, the three remaining equations are satisfied by

$$\omega_1 = \pm\left[\left(\frac{H}{I_2}\right)^2 - \left(\frac{I_3\omega_3}{I_1 - I_3^p}\right)^2\right]^{1/2}, \qquad \omega_2 = 0$$

$$\omega_3^p = \left(\frac{I_3}{I_1 - I_3^p}\right)\omega_3, \qquad \omega_3 = \omega_0 + \frac{(T_J + T_M)t}{I_3} \tag{24a}$$

where $\lambda = 1/I_1$. For $I_1 < I_2$, or $\mu < 0$, these equations are satisfied by

$$\omega_1 = 0, \qquad \omega_2 = \pm\left[\left(\frac{H}{I_2}\right)^2 - \left(\frac{I_3\omega_3}{I_2 - I_3^p}\right)^2\right]^{1/2}, \qquad \omega_2 = 0$$

$$\omega_3^p = \left(\frac{I_3}{I_2 - I_3^p}\right)\omega_3, \qquad \omega_3 = \omega_0 + \frac{(T_J + T_M)t}{I_3} \tag{24b}$$

where $\lambda = 1/I_2$. From a similar argument as before, the following condition has to be satisfied,

$$\frac{I_3}{I_i - I_3^p} < 1 \qquad i = 1 \text{ for } I_1 > I_2, \quad i = 2 \text{ for } I_1 < I_2 \tag{24c}$$

Equation (24c) is less likely to be met by spacecraft, since most spacecraft have a more massive rotor, such that the value of I_3 is more comparable with that of I_t. In general, I_3^p is only a factor of half of that of I_t or less. At first sight, it would be expected that a similar switch-over behavior will also occur for the platform resonance, but in fact a detailed parametric sweep (not shown) through the full simulations does not seem to indicate the existence of such a switch. In fact, the stability equation is now

$$\delta^2 L = \tfrac{1}{2}[I_1(1 - \lambda I_1)(\omega_1 - \omega_1^{(s)})^2 + I_2(1 - \lambda I_2)(\omega_2 - \omega_2^{(s)})^2 + I_3(1 - \lambda I_3^p)(\omega_3^p - \omega_3^{p(s)})^2] \tag{25}$$

By substituting the rates of Eqs. (24a) and (24b) into Eq. (25), it can be shown that the latter is positive definite, implying that the stationary point is a local energy minimum. Now, from Eqs. (24), the nonvanishing transverse rate component corresponds to the larger, rather than the smaller, transverse inertia. The state corresponding to this local minimum trap is realizable in principle; however, it has not been discovered from the full simulation results over a wide range of parameters and initial conditions. Convergence to such a trap might require disabling the motor or the jet torque near the trap, which has not been attempted in this study.

Third, let us briefly remark on the more general dual spinners that have dynamic asymmetries in both bodies. It can be shown from Eqs. (2–4b), that

$$I_1 = I_t + [I_t^{(r)}\Delta_r + I_t^{(n)}\Delta_n(c^2 - s^2)] \tag{26a}$$

$$I_2 = I_t - [I_t^{(r)}\Delta_r + I_t^{(n)}\Delta_n(c^2 - s^2)] \tag{26b}$$

where $I_1^{(x)} = I_t^{(x)}(1 + \Delta_x)$ and $I_2^{(x)} = I_t^{(x)}(1 - \Delta_x)$, $x = r, n$ and $I_t^{(r)} + I_t^{(n)} = I_t$. In this case, a saddle point transition can occur even for the platform resonance if the rotor asymmetry is large enough. From Eqs. (26), the nonresonant body contribution to the asymmetry has alternate signs in time, thus, $\delta^2 L$ of Eq. (25) cannot be positive definite. A saddle point transition may still occur. Indeed, a saddle transition that appears qualitatively similar to the one described earlier in the rotor resonance has been observed in some simulations of the platform resonance with large rotor asymmetry (results not presented here due to space limitations).

V. Conclusions

The foregoing analysis provides a unifying treatment of the linear theory of despin resonance of the rotor and the platform of a dual-spin spacecraft with free nutation. The linear model is developed in the spirit of simplicity. However, the model is capable of capturing the major qualitative features of the phenomena. The model is shown to depend on three essential nondimensional parameters that quantify: 1) the degree of dynamic imbalance of the resonant body, 2) the degree of asymmetry of the resonant body, and 3) the time duration from start of the maneuver to the state of maximal coning. For the sake of simplicity, the nonresonant body has been assumed symmetric and balanced throughout. The linear analysis is supplemented by a simple variational nonlinear analysis. Such a nonlinear approach allows certain quasistationary points to be isolated from the phase space. These points may be encountered by the trajectory of the state during despin. A stability check of these points shows that they are either saddle points or local minima. An example of a transition through a saddle point from the fully nonlinear simulation of a despin maneuver has been provided. Such a transition has been called the stall condition in spacecraft maneuvers. The phase state of such a transition for the analytical and the simulation results agree reasonably well.

Acknowledgments

The study was stimulated by the fully nonlinear despin simulation results on several spacecraft that exhibit one or the other type of the resonances. I am grateful to S. C. Jennings, W. S. Sargent, and J. J. McEnnan for their valuable discussions.

References

[1]Velman, J. R., and Belardi, J. W., "Gyrostat Attitude Dynamics," Hughes Aircraft Company, Los Angeles, CA, SSD 90159R, May 1969.

[2]Scher, M. P., and Farrenkopf, R. L., "Dynamic Trap States of Dual Spin Spacecraft," *AIAA Journal,* Vol. 12, No. 12, 1974, pp. 1721–1725.

[3]Cochran, J. E., "Nonlinear Resonances in the Attitude Motion of Dual-Spin Spacecraft," *Journal of Spacecraft and Rockets,* Vol. 14, No. 9, 1977, pp. 562–572.

[4]Adams, G. J., "Dual-Spin Spacecraft Dynamics During Platform Spinup," *Journal of Guidance, Control, and Dynamics,* Vol. 3, No. 1, 1980, pp. 29–36.

[5]Hollars, M. G., "Minimum Energy Trap States of Dual-Spin Spacecraft," *Journal of Guidance, Control, and Dynamics,* Vol. 5, No. 3, 1982, pp. 286–290.

[6]Lebsock, K. L., "Despin Through Unity Inertia Ratio," *Journal of Astronautical Sciences,* Vol. 30, No. 3, 1982, pp. 213–227.

[7]Tsuchiya, K., "Attitude Behavior of a Dual-Spin Spacecraft Composed of Asymmetric Bodies," *Journal of Guidance and Control,* Vol. 2, July–Aug. 1979, pp. 328–333.

[8]Lukich, M. L., and Mingori, D. L., "Attitude Stability of Dual-Spin Spacecraft with Unsymmetrical Bodies," *Journal of Guidance, Control, and Dynamics,* Vol. 8, No. 1, 1985, pp. 110–117.

[9]Likins, P. W., "Attitude Stability for Dual-Spin Spacecraft," *Journal of Spacecraft and Rockets,* Vol. 4, No. 12, 1967, pp. 1638–1643.

[10]"Advanced Continuous Simulation Language (ACSL)," Reference Manual, Mitchell and Gauthier Associates, Concord, MA, 1986.

[11]Hughes, P. C., *Spacecraft Attitude Dynamics,* Wiley, New York, 1986.

[12]Kane, T. R., and Levinson, D. A., "Energy-Sink Analysis of System Containing Driven Rotors," *Journal of Guidance, Control, and Dynamics,* Vol. 3, No. 3, 1980, pp. 334–338.